Reprinted from January 1988, Vol. 110, Journal of Turbomachinery

Film Cooling and Heat Transfer in Nozzles

J. Stoll

J. Straub

Lehrstuhl A für Thermodynamik,
Technische Universität München,
Munich, Federal Republic of Germany

In this paper experimental and theoretical investigations on heat transfer and cooling film stability in a convergent-divergent nozzle are presented. Compressed air is injected into hot air in the inlet region of the nozzle and the influence of the strong favorable pressure gradient in the nozzle on turbulent heat transfer and mixing is examined. The experiments cover measurements of wall pressures, wall temperature, and wall heat flux. Calculations with parabolic finite difference boundary layer code have been performed using a well-known k-ϵ-turbulence model with an extension paying regard to acceleration. As a result the calculated wall heat flux is compared with the measured heat flux.

Introduction

Some authors have already worked on heat transfer in nozzles (e.g., Back et al., 1964, 1970, 1972; Boldmar et al., 1967, 1972; Winkler and Grigull, 1977; Bauer et al., 1977, 1978) and an increasing number of investigations has been undertaken on heat transfer in accelerated compressible flow (e.g., Kays et al., 1970; Blair, 1982; Wang et al., 1985; Rued and Wittig, 1985).

Much fundamental research has been done considering the injection geometry and the stability of cooling films. Many publications have dealt with the comparison of adiabatic and isothermic wall experiments trying to generalize the results using scaling laws (Jones and Forth, 1986) and trying to generalize the results using dimensionless variables based on recovery temperatures (Ligrani and Camci, 1985) and giving density ratio and variable property corrections in the case of compressible flow.

Only a few authors have examined the influence of mainstream pressure gradients on heat transfer to film-cooled surfaces (Hay et al., 1985). Heat transfer to a film-cooled nozzle wall is as much influenced by the strong favorable pressure gradient as by large density ratio. Furthermore the recovery temperature of both the hot gas and the coolant are submitted to substantial changes in the streamwise direction. Therefore a presentation of our test results in nondimensional form would not allow for generalization.

In order to generalize results, it is important to test and improve existing computer codes in comparison with experimental data. The work on comparison of finite difference codes for prediction of heat transfer to film-cooled surfaces (Crawford, 1986) is still continuing. In the present investigation we compare calculations with a low Reynolds number k-ϵ model (Lam and Bremhorst, 1981) modified for accelerated flows to our experiments.

Contributed by the Gas Turbine Division of THE AMERICAN SOCIETY OF MECHANICAL ENGINEERS and presented at the 32nd International Gas Turbine Conference and Exhibit, Anaheim, California, May 31-June 4, 1987. Manuscript received at ASME Headquarters February 10, 1987. Paper No. 87-GT-117.

Experiments

Experimental Setup. The experimental investigations have been performed in the wind tunnel of our institute. Compressed air is used both as hot medium and as coolant. The hot air is compressed in a two-stage radial compressor to a maximum stagnation pressure of 0.28 MPa and a maximum stagnation temperature of 485 K. The hot air passes a mixer, a straightener, and a transition pipe, where the cross section is changed from a round to a rectangular one of nearly the same area before it enters the test section with 2.8 kg/s maximum mass flow rate.

The cooling air is compressed in a smaller two-stage compressor with intermediate heat exchanger. It enters the test section with a stagnation temperature of approximately 305 K and a maximum mass flow rate of 0.25 kg/s. The whole apparatus is driven in steady state.

Test Section. The test section is an asymmetric rectangular water-cooled CD nozzle (Fig. 1), which is designed for a normal shock at its exit in the maximum loading case of the compressor allowing a maximum outlet Mach number of 2.25. The geometry of the rectangular test section in the x, y plane is shown in Fig. 1. The depth normal to Fig. 1 is 99 mm (Fig. 3) avoiding serious three-dimensional effects. The rectangular 30 deg–15 deg semiangle convergent-divergent nozzle is constructed with a plane and a contoured wall. Thus it is possible to examine the influence of the favorable pressure gradient in the absence of effects of wall curvature.

The nozzle was built up with 35 separately water-cooled segments (Fig. 3) of copper on each of the two side walls to allow very accurate measurements of the heat flux from the air to the nozzle walls. By adjusting the cooling water flow rate for each segment it is possible to establish a defined thermal boundary condition. The segments are well insulated from each other by air and a thin stainless steel tube at the nozzle surface. The gas side nozzle walls have been chrome plated in order to avoid oxidation and to reduce thermal radiation. The average surface roughness has been determined as 7.3 ± 1.3 μm.

The mass flux ratio in the case of the film cooling experiments is defined by varying the hot air mass flow and the

cooling air mass flow for different slot heights for the cooling film. The inlet region of the nozzle with inlet geometry is shown in Fig. 2.

Measurement Techniques. The experimental investigation covers measurements of wall temperature, wall heat flux, wall pressures, stagnation pressure and temperature and measurements of the mass flow rates. Wall temperature and wall heat flux were measured with the heat flux meters as shown in Fig. 2 using two thermocouples installed in the copper segments. Under steady-state conditions the wall heat flux and the wall temperature are calculated from the one-dimensional heat conduction equation. Two-dimensional finite element calculations for the copper segments have proved the high accuracy of this simple method. The thermocouples are connected to a scanner and a digital voltmeter.

The wall pressures are taken from the small steel tubes between the copper segments and transferred to a Scanivalve pressure scanning system. Total pressures and total temperatures are taken from combined probes.

The mass flow rate of the hot air is calculated from one-dimensional gas dynamics relations in the absence of a cooling film. The mass flow rate of the cold air is measured with a standard orifice. The inlet velocities are calculated from the inlet geometry (Figs. 2 and 3). An HP 1000 Minicomputer was used to acquire the data from the pressure scanning system and the digital voltmeter during the test run, allowing immediate evaluation of the mass flow rates and the distribution of pressure, wall temperature, and wall heat flux. By using the computer for continuously evaluating the wall temperature and the wall heat flux during scanning, it was possible to establish isothermal wall conditions by manually adjusting the cooling water control in an acceptable time.

Calculations

Mean Flow Equations. The mean flow equations have been derived from the conservation equations using Favre mass-averaged decomposition, thus keeping the correlation terms arising from density fluctuations to a minimum and maintaining almost the same forms as the equations written for incompressible flows (Favre, 1965, 1975; Vandrome and Minh, 1984). Additional density fluctuation correlations remain unmodeled in this presentation; they are omitted right from the very beginning. The equations are given in general coordinates for stationary conditions. The mathematical notations for operators and operations in general coordinates is defined in (Klingbeil, 1966).

Continuity equation

$$\text{div}\,(\bar{\rho}\tilde{\mathbf{w}}) = 0 \tag{1}$$

Momentum equations

$$\mathbf{Div}\,(\bar{\rho}\tilde{\mathbf{w}}\tilde{\mathbf{w}}) = -\,\mathbf{grad}\,\bar{p} + \mathbf{Div}\bar{\tau} + \mathbf{Div}(-\bar{\rho}\widetilde{\mathbf{w}''\mathbf{w}''}) \tag{2}$$

Total enthalpy equation

$$\text{div}(\bar{\rho}\tilde{\mathbf{w}}\tilde{H}) = \text{div}(\lambda\,\mathbf{grad}\,\tilde{T}) + \text{div}(\overline{\tau\cdot\mathbf{w}}) + \text{div}(-\bar{\rho}\widetilde{\mathbf{w}''H''}) \tag{3}$$

$$\tilde{H} = \tilde{h} + \frac{\tilde{\mathbf{w}}\cdot\tilde{\mathbf{w}}}{2} + \frac{\widetilde{\mathbf{w}''\cdot\mathbf{w}''}}{2} = \tilde{h} + \frac{\tilde{\mathbf{w}}\cdot\tilde{\mathbf{w}}}{2} + k \tag{4}$$

$$H'' = h'' + \tilde{\mathbf{w}}\cdot\mathbf{w}'' + \frac{\mathbf{w}''\cdot\mathbf{w}''}{2} - \frac{\widetilde{\mathbf{w}''\cdot\mathbf{w}''}}{2} \tag{5}$$

Assuming an ideal gas, the connection between the variables is given by the ideal gas law

$$\bar{p} = \bar{\rho}R\tilde{T} \tag{6}$$

and the equation of state for the enthalpy

$$d\tilde{h} = c_p d\tilde{T} \tag{7}$$

Turbulent Transport. Neglecting turbulent diffusive

Nomenclature

c_p = specific heat at constant pressure
C_μ, C_1, C_2, C_3 = turbulence model constants
f_μ, f_1, f_2, f_3 = turbulence model wall functions
f = wall function = min $(R_t/3.72\,R_k, 1.)$
H = total enthalpy
h = specific enthalpy
$\mathbf{I}$ = unity tensor
k = turbulent kinetic energy
K = acceleration parameter $= -(\mu/\rho^2 u_\infty^2)(\partial p/\partial x)$
l = turbulent mixing length
$\dot{m}$ = mass flow
p = pressure
Pr_t = turbulent Prandtl number $= \mu_t c_p/\lambda_t$
R = gas constant
Re_k = turbulence Reynolds number $= k^2\rho/\epsilon\mu$
Re_t = turbulence Reynolds number $= \sqrt{k}y\rho/\mu$
Re_l = turbulence Reynolds number $= \sqrt{k}l\rho/\mu$
s = slot height
T = temperature
u = mean velocity in streamwise direction
u_τ = friction velocity $= (\mu_w/\rho_w)(\partial u/\partial y)$
u'', v'', w'' = fluctuating velocities in x, y, z directions
$\mathbf{w}$ = velocity vector in general coordinates
x, y, z = quasi-orthogonal streamwise coordinates
x = streamwise direction; distance from slot
y = cross-stream coordinate; distance from wall
z = coordinate parallel to the wall
x_t = distance from turbulence grid
Δy = stream tube width
Δx^+ = dimensionless streamwise step $= \Delta x u_\tau(\rho_w/\mu_w)$
y^+ = dimensionless wall distance $= y u_\tau(\rho_w/\mu_w)$
δ = boundary layer thickness
ϵ = turbulent dissipation rate $= (1/\bar{\rho})\,\boldsymbol{\tau}'':\mathbf{Grad}\,\mathbf{w}''$
λ = thermal conductivity
μ = dynamic viscosity
ν = kinematic viscosity $= \mu/\rho$
ρ = density
σ_ϵ = turbulent diffusion Prandtl number for turbulent dissipation rate
τ = shear stress
$\boldsymbol{\tau}$ = stress tensor $= \mu\{\mathbf{Grad}\,\mathbf{w} + (\mathbf{Grad}\,\mathbf{w})^T - (2/3)\,\text{div}\,(\mathbf{w})\mathbf{I}\}$

Subscripts and Superscripts

$\bar{}$ = denotes time-averaged value
$\tilde{}$ = denotes mass-averaged mean value
$''$ = denotes fluctuating part of variable
0 = denotes stagnation condition
c = coolant
w = wall
∞ = free stream
r = recovery condition
t = turbulent

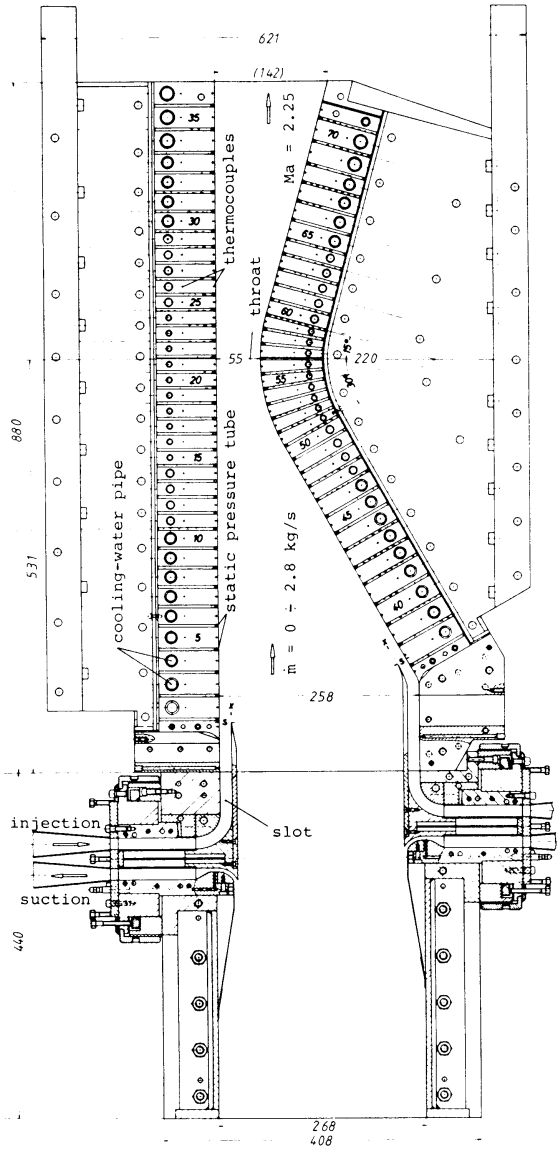

Fig. 1 Test section

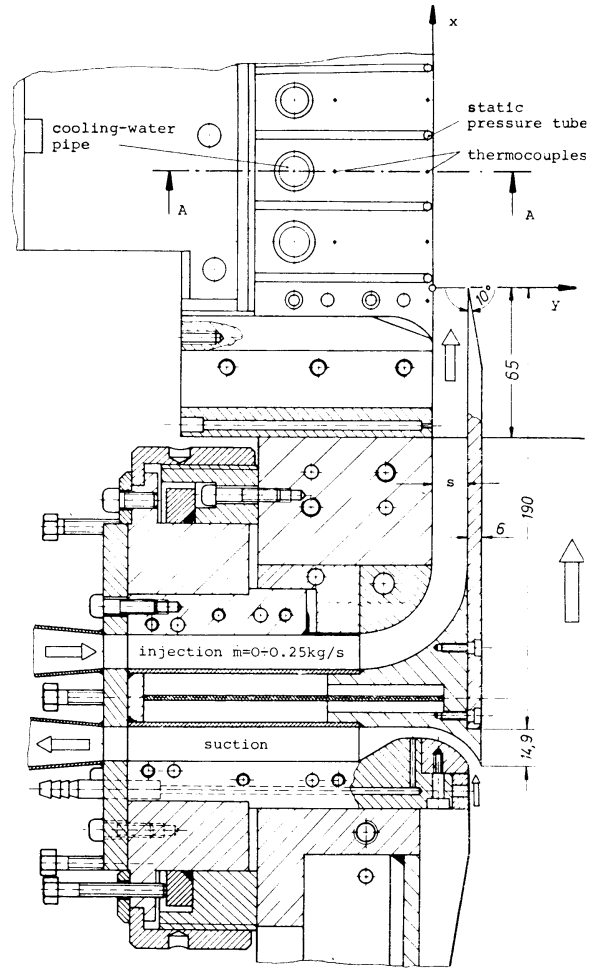

Fig. 2 Inlet geometry

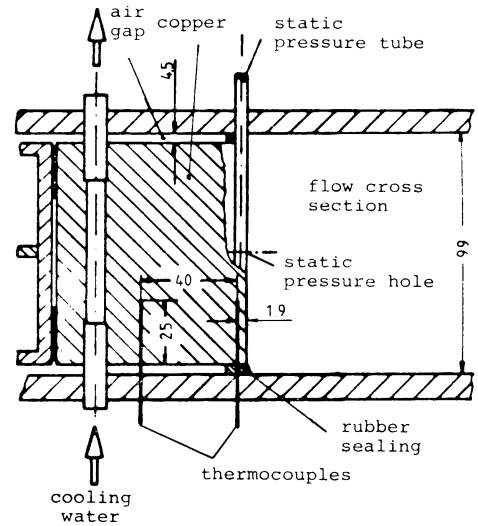

Fig. 3 Sectional view; copper segment

transport in the streamwise direction, the reduced boundary layer equations contain only two important terms: $-\tilde{\rho}\widetilde{u''v''}$ and $-\tilde{\rho}\widetilde{v''H''}$. The turbulent stress $-\tilde{\rho}\widetilde{u''v''}$ in the momentum equation and the turbulent total enthalpy flux $-\tilde{\rho}\widetilde{v''H''}$ in the total enthalpy equation are modeled using the eddy viscosity concept

$$-\tilde{\rho}\widetilde{u''v''} = \mu_t \frac{\partial u}{\partial y} \tag{8}$$

and after rearranging

$$-\tilde{\rho}\widetilde{v''H''} = -\tilde{\rho}\widetilde{v''h''} - \tilde{u}\tilde{\rho}\widetilde{u''v''} - \tilde{\rho}\widetilde{v''k''} \tag{9}$$

The eddy diffusivity concept for the turbulent heat flux is

$$-\tilde{\rho}\widetilde{v''h''} = \lambda_t \frac{\partial \tilde{T}}{\partial y} = \frac{\lambda_t}{c_p}\frac{\partial \tilde{h}}{\partial y} \tag{10}$$

and for the flux of turbulent kinetic energy it is

$$-\tilde{\rho}\widetilde{v''k''} = \mu_t \frac{\partial k}{\partial y} \tag{11}$$

The equation for the total enthalpy flux may now be written

$$-\tilde{\rho}\widetilde{v''H''} = \frac{\lambda_t}{c_p}\frac{\partial \tilde{H}}{\partial y} + \left(\mu_t - \frac{\mu_t}{\mathrm{Pr}_t}\right)\left\{\frac{\partial(\tilde{u}^2/2)}{\partial y} + \frac{\partial k}{\partial y}\right\} \tag{12}$$

where Pr_t is a turbulent Prandtl number relating the turbulent conductivity λ_t to the turbulent viscosity μ_t. The turbulent viscosity μ_t is assumed to be proportional to a turbulence velocity scale and a turbulence length scale. Following the proposal of Jones and Launder (1972) the turbulence viscosity may be obtained from

$$\mu_t = C_\mu f_\mu \tilde{\rho}\frac{k^2}{\epsilon} \tag{13}$$

where ϵ is the turbulent dissipation rate; C_μ is a constant and f_μ is a function introduced to account for viscous effects in the near wall region.

The k-ϵ Model. The transport equations for k and ϵ originally derived from the momentum equations are given in modeled form (Jones and Launder, 1972; Lam and Bremhorst, 1981). Although the ϵ equation can be derived with the assumption $\nu_t = \mu_t/\rho = \text{const}$, it has beeen widely used for variable property flows (Hein et al. 1980; Vandromme and Minh, 1984; Rodi and Scheurer, 1985).

Turbulent energy equation

$$\text{div}\,(\bar{\rho}\tilde{\mathbf{w}}k) = \text{div}((\mu+\mu_t)\,\mathbf{grad}\,k) + P_k - \bar{\rho}\epsilon \tag{14}$$

$$P_k = -\bar{\rho}\widetilde{\mathbf{w}''\mathbf{w}''} : \mathbf{Grad}\,\tilde{\mathbf{w}} \tag{15}$$

$$\bar{\rho}\epsilon = \overline{\tau'' : \mathbf{Grad}\,\mathbf{w}''} \tag{16}$$

Turbulent dissipation rate equation

$$\text{div}(\bar{\rho}\tilde{\mathbf{w}}\epsilon) = \text{div}\left(\left(\mu + \frac{\mu_t}{\sigma_\epsilon}\right)\mathbf{grad}\epsilon\right) + C_1 f_1 \frac{\epsilon}{k} P_k - C_2 f_2 \bar{\rho}\frac{\epsilon^2}{k} + P_\epsilon \tag{17}$$

$$P_\epsilon = -2\overline{\tau'' : \{\mathbf{Grad}\,\tilde{\mathbf{w}} \cdot \mathbf{Grad}\,\mathbf{w}'' + \mathbf{Grad}\,\mathbf{w}'' \cdot \mathbf{Grad}\,\tilde{\mathbf{w}}\}} \tag{18}$$

$$-2\overline{\tau'' : \{\mathbf{w}'' \cdot \mathbf{Grad}\,(\mathbf{Grad}\,\tilde{\mathbf{w}})\}} \tag{19}$$

The generation terms P_k and P_ϵ are written in their original form first to give attention to effects of acceleration. For the production of turbulent energy in a boundary layer the use of streamline quasi-orthogonal coordinates leads to

$$P_k = -\bar{\rho}\widetilde{u''v''}\frac{\partial \tilde{u}}{\partial y} - \rho\widetilde{u''u''}\frac{\partial u}{\partial x} - \bar{\rho}\widetilde{v''v''}\tilde{u}\Gamma^2_{21} \tag{20}$$

where Γ^2_{21} is one of the Christoffel symbols arising from tensor analysis and might be interpreted as a measure of stream tube growth; $\Gamma^2_{21} \approx (1/\Delta y)(\partial \Delta y/\partial x)$ (Γ^1_{11} is neglected; $\Gamma^1_{11} \approx 0$).

Elimination of Γ^2_{21} using the equation of continuity yields

$$P_k = -\bar{\rho}\widetilde{u''v''}\frac{\partial \tilde{u}}{\partial y} - (\bar{\rho}\widetilde{u''u''} - \bar{\rho}\widetilde{v''v''})\frac{\partial \tilde{u}}{\partial x} + \widetilde{v''v''}\tilde{u}\frac{\partial \bar{\rho}}{\partial x} \tag{21}$$

which is consistent with Hanjalic and Launder (1980), Rodi and Scheurer (1983), and Back et al. (1964) except for the variable density term being important in the supersonic region. The first term of P_k is the most important one in a boundary layer and is obtained without additional modeling assumptions

$$-\bar{\rho}\widetilde{u''v''}\frac{\partial \tilde{u}}{\partial y} = \mu_t\left(\frac{\partial \tilde{u}}{\partial y}\right)^2 \tag{22}$$

Concerning the remaining terms of P_k, it is better to retain the view of P_k being an exchange term between the energy of turbulent motion and mean flow appearing with reverse sign in the equation of mechancial energy of the mean flow. In the case of a boundary layer ($\widetilde{u''u''} > \widetilde{v''v''}$) in an accelerated flow ($\partial\tilde{u}/\partial x > 0$, $\partial\bar{\rho}/\partial x < 0$) the remaining terms of P_k are always negative, transferring turbulent kinetic energy to mechanical energy of the mean flow.

The acceleration terms are an order of magnitude smaller than the production P_k but the small imbalance $P_k - \bar{\rho}\epsilon$ is influenced effectively. However, it would be hasty to rush to the conclusion that there is a decay of turbulent viscosity in an accelerated flow leaving the turbulent dissipation rate unconsidered. There is a quite similar behavior of the term P_ϵ in the dissipation rate equation and the ideal for modeling is already given by Hanjalic and Launder (1972). If the increase of the standard production of ϵ in the low Reynolds number region (Kebede et al., 1985) is assumed to be already considered when introducing the f_1 function, and

$$-2\overline{\tau'' : \{\mathbf{w}'' \cdot \mathbf{Grad}(\mathbf{Grad}\,\tilde{\mathbf{w}})\}} \tag{23}$$

is neglected, as in the standard model (Lam and Bremhorst, 1981), P_ϵ reduces to the transfer term

$$P_\epsilon = -2\overline{\tau'' : \begin{pmatrix} 2\dfrac{\partial u''}{\partial x}\dfrac{\partial \tilde{u}}{\partial x} & \dfrac{\partial v''}{\partial x}\,\text{div}\,\tilde{\mathbf{w}} & \dfrac{\partial w''}{\partial x}\dfrac{\partial \tilde{u}}{\partial x} \\ \dfrac{\partial u''}{\partial y}\,\text{div}\,\tilde{\mathbf{w}} & 2\dfrac{\partial v''}{\partial y}\,\tilde{u}\Gamma^2_{21} & \dfrac{\partial w''}{\partial y}\tilde{u}\Gamma^2_{21} \\ \dfrac{\partial u''}{\partial z}\dfrac{\partial \tilde{u}}{\partial x} & \dfrac{\partial v''}{\partial z}\tilde{u}\Gamma^2_{21} & 0 \end{pmatrix}} \tag{24}$$

with

$$\text{div}\,\tilde{\mathbf{w}} = \frac{\partial \tilde{u}}{\partial x} + \tilde{u}\Gamma^2_{21} \tag{25}$$

Since the transfer term contains components of

$$\bar{\rho}\epsilon = \overline{\tau'' : \mathbf{Grad}\,\mathbf{w}''} = \tau' : \overline{\begin{pmatrix} \dfrac{\partial u''}{\partial x} & \dfrac{\partial v''}{\partial x} & \dfrac{\partial w''}{\partial x} \\ \dfrac{\partial u''}{\partial y} & \dfrac{\partial v''}{\partial y} & \dfrac{\partial w''}{\partial y} \\ \dfrac{\partial u''}{\partial z} & \dfrac{\partial v''}{\partial z} & \dfrac{\partial w''}{\partial z} \end{pmatrix}} \tag{26}$$

it seems reasonable to model the transfer term proportional to the dissipation rate and the acceleration of the flow. In the present calculations, we used the compressible analogy to the relation (Hanjalic and Launder, 1980; Rodi and Scheurer, 1983)

$$P_\epsilon = -C_3 f_3 \frac{\epsilon}{k}\left\{\bar{\rho}(\widetilde{u''u''} - \widetilde{v''v''})\frac{\partial \tilde{u}}{\partial x} - \widetilde{v''v''}\tilde{u}\frac{\partial \bar{\rho}}{\partial x}\right\} \tag{27}$$

although the dependence on $\widetilde{u''u''}$, $\widetilde{v''v'}$, and $\tilde{u}(\partial\bar{\rho}/\partial x)$ might be a subject for further discussion.

The constants and wall functions in the turbulence model equations (13), (14), (17), (21), and (27) are taken from Lam and Bremhorst (1981)

$$C_\mu = 0.09 \quad f_\mu = (1 - e^{-0.0165\text{Re}_k})^2\left(1 + \frac{20.5}{\text{Re}_t}\right) \tag{28}$$

$$\sigma_\epsilon = 1.3 \tag{29}$$

$$C_1 = 1.44 \quad f_1 = 1 + \left(\frac{0.05}{f_\mu}\right)^3 \tag{30}$$

$$C_2 = 1.92 \quad f_2 = 1 - e^{-\text{Re}_t^2} \tag{31}$$

$$\text{Re}_t = \frac{k^2\rho}{\epsilon\mu} \quad \text{Re}_k = \frac{\sqrt{k}y\rho}{\mu} \tag{32}$$

Very little is known about the turbulence quantities $\widetilde{u''u''}$ and $\widetilde{v''v''}$ in accelerated flows appearing in the transfer terms in the turbulent transport equations. In accordance with measurements in zero pressure gradient flow, a turbulence structure coefficient for $\widetilde{u''u''}$ was used with a fixed value

$$\frac{\widetilde{u''u''}}{k} = 1 \tag{33}$$

and $\widetilde{v''v''}$ was calculated from a standard relation (e.g., Ljuboja and Rodi, 1981; Gibson, 1978) with the additional assumption $P_k \approx \bar{\rho}\epsilon$

$$\frac{\widetilde{v''v''}}{k} = 0.52\left(\frac{1-0.25\,f}{1+0.667f}\right) \tag{34}$$

For the additional constant in the dissipation rate equation we used

$$C_3 = 4.44 \quad f_3 = 1 \tag{35}$$

as originally given by Hanjalic and Launder (1980).

For the turbulent Prandtl number the equation

$$\mathrm{Pr}_t = 0.67\,\frac{1+0.675\,f}{1+0.5\,f}\,(1+0.167\,f) \tag{36}$$

is used as developed by Ljuboja and Rodi (1981) from an analysis of the $\widetilde{v''T''}$ equation. In a boundary layer

$$f = \frac{\mathrm{Re}_t}{3.72\mathrm{Re}_k} = \frac{k^{3/2}}{3.72\epsilon y} \approx \frac{(-\widetilde{u''v''})^{3/2}}{0.41\epsilon y} = \frac{L}{0.41y} = 1 \tag{37}$$

yields $\mathrm{Pr}_t = 0.86$ as used in most calculations. In the outer region $f \to 0$ leads to $\mathrm{Pr}_t = 0.67$, which is consistent with some measurements (Townsend, 1976). The equation for Pr_t was used without modifications in the present calculations although other measurements (Fiedler, 1974; Chambers et al., 1985) indicate that the turbulent Prandtl number in a turbulent mixing layer should be even lower, e.g., $\mathrm{Pr}_t \approx 0.5$, calling for a change of constants in the Pr_t formula.

Initial and Boundary Conditions

Boundary Conditions. The wall pressures obtained from the experiments were used as a boundary condition for the calculations performed with the parabolic finite difference code. In the absence of curvature effects a cross-stream zero pressure gradient was assumed in the present calculations. The assumption of negligible curvature is also valid in the case of film cooling for velocity ratios less than 3 (Abramovich, 1963). The measured wall temperatures were used as the thermal boundary condition, and the calculated wall heat flux is compared with the measured heat flux.

Velocity and kinetic energy were set to zero at the wall, and the dissipation rate of turbulent kinetic energy at the wall was calculated from the reduced turbulent kinetic energy equation

$$\epsilon_w = \frac{\mu}{\rho}\left(\frac{\partial^2 k}{\partial y^2}\right)_w \tag{38}$$

All variables were submitted to a vanishing cross-stream gradient as a free-stream boundary condition. In the absence of cross-stream diffusive transport the mean flow equations reproduce the isentropic relation, and the turbulence transport equations automatically reduce to the decay equations

$$u_\infty \frac{\partial k}{\partial x} = -\epsilon \tag{39}$$

$$u_\infty \frac{\partial \epsilon}{\partial x} = -C_2 \frac{\epsilon^2}{k} \tag{40}$$

Initial Conditions. As initial velocity profiles, the profile for a zero pressure gradient boundary layer developed on the surface from the suction to the coolant entry (Fig. 2) was used for the hot gas, and a velocity profile for fully delevoped channel flow was used for the cooling film. The mass flux of the coolant and the free-stream velocity were obtained from the experiment. Since the slot was not removed in the absence of coolant injection, we assumed a slightly smaller initial boundary layer thickness. In the near-wall regions the velocity profiles were determined by the law of the viscous sublayer.

The temperature profiles were obtained from the generalized Crocco relation

$$T = T_w + (T_r - T_w)\,\frac{u}{u_\infty} - r\,\frac{u^2}{2\,c_p} \tag{41}$$

$$r = 0.88 \tag{42}$$

In the fully turbulent region the turbulent kinetic energy of the hot gas boundary layer is obtained from

$$k = \frac{\tau}{\sqrt{c_\mu \rho}} \tag{43}$$

with an additional wall damping correction.

The turbulent mixing length is defined by the ramp function $l = \min(0.41y,\ \mu\delta)$, with λ as defined by Crawford and Kays (1976). The turbulent dissipation rate is calculated from (Norris, 1975)

$$\epsilon = C_\mu^{1/4}\,\frac{k^{3/2}}{l}\left(1+\frac{1.9}{\mathrm{Re}_l}\right) \tag{44}$$

A smooth distribution of all variables between fully turbulent region and free stream was obtained using the Wake function

$$W\left(\frac{y}{\delta}\right) = 2\left(3\left(\frac{y}{\delta}\right)^2 - 2\left(\frac{y}{\delta}\right)^3\right) \tag{45}$$

The free-stream value of the turbulent kinetic energy was obtained from $k_\infty = 3/2\ Tu_\infty^2 u_\infty^2$ with $Tu_\infty = 1.5$ percent from the experiments of Bauer et al. (1980) in the same test section. The free-stream dissipation rate of turbulent energy was calculated from the decay of grid turbulence

$$\epsilon_\infty = \frac{u_\infty k_\infty}{c_2 - 1}\,\frac{1}{x_t} \qquad x_t = 0.5 \text{ m} \tag{46}$$

The turbulent kinetic energy at the entry of the cooling film was fixed at 5 percent.

Solution Procedure

The mean flow equations for momentum and total enthalpy and the transport equations for turbulent energy and turbulent dissipation rate were solved on a streamline grid with a new computer code developed by the authors. The finite difference equations were obtained by integrating the differential equations over the grid defined control volume according to the Gaussian integration rule

$$\int\int_V \int \text{div } \mathbf{vector}\ dV = \int_S \int \mathbf{vector}\cdot\mathbf{n}\ dS \tag{47}$$

where V = control volume; S = surface of control volume; $\mathbf{n}$ = unity vector normal to the surface. Thus conservation of convective and diffusive transport is guaranteed automatically. The usual ω transformation (Patankar and Spalding, 1970; Crawford and Kays, 1976) is omitted for simplicity and more attention to the slowly varying region of the viscous sublayer.

The finite difference equations are solved fully implicit in the streamwise direction without iteration and interpolation for the boundary conditions.

In order to obtain grid-independent solutions a nonequidistant grid with 100 nodes was established in the cross-stream direction with a constant spreading rate of 1.1 at the starting location. The first grid node away from the wall was at a distance of $y^+ = 0.1$ approximately constant during the whole calculation. A constant forward step $\Delta x = 10^{-3}$ m was chosen in the present calculations, giving a nondimensional step size of $300 < \Delta x^+ < 1000$. The results remained unchanged for smaller step size. The calculation time per forward step was 0.025 s on a CDC Cyber 875 and the total computing time was 20 s per run.

The independence of the results from the calculation procedure has been examined in comparison with a modified ver-

sion of the GENMIX computer code (Patankar and Spalding, 1970).

Results

Heat transfer and film cooling have been studied for four different mainstream conditions. Mass flow, stagnation pressure, stagnation temperature, average entry velocity, and isothermal wall temperature for the heat transfer experiments are given in Table 1.

The measured pressures along the flat side of the nozzle are shown in Fig. 4. The acceleration parameter K is of the order 10^{-6} and a typical value at the throat is 0.3×10^{-6}. The wall heat flux measurements are plotted in Fig. 5 in comparison with the results calculated with the finite difference code.

In the case of film cooling, heat transfer results are shown for two mainsteam conditions in Figs. 7, 9, 11, and 13 for different coolant mass flow rates. The wall heat flux is plotted again in comparison with the finite difference calculations and the measured wall temperatures used as thermal boundary condition of the calculations are given in Figs. 6, 8, and 10, and 12.

Injection mass flow, mass flow ratio, mass flux ratio, momentum flux ratio, injection velocity ratio, average injection velocity, injection temperature, and temperature ratio at the entry of the injected cold air are given in Tables 2–5.

Conclusions

Experiments and calculations on heat transfer and film cooling stability in a convergent-divergent nozzle are presented.

Heat Transfer. The maximum wall heat flux is determined slightly upstream from the throat as indicated in earlier measurements. In contrast to many simple correlation methods finite difference calculations predict the location of the maximum very well, but most standard turbulence models (e.g., Crawford and Kays, 1976; Norris, 1975; Norris and Reynolds, 1975; Jones and Launder, 1972; Lam and Bremhorst, 1981; Chien, 1982) underpredict the wall heat flux by approximately 10 percent. The underprediction of heat transfer has also been observed by Crawford (1986) comparing calculations with WR (Wilcox and Rubesin, 1980), JL (Jones and Launder, 1972) and CH (Chien, 1982) and two-equation turbulence models with the favorable pressure gradient experiments of (Julien et al., 1969; Theilbar et al., 1969). Kays et al. (1970) have used a zero-equation model very similar to the STAN5 zero-equation model (Crawford and Kays, 1976), but with a higher Karman constant (0.44) in comparison to their measurements of the heat transfer to a highly accelerated turbulent boundary layer. This modification also improves the agreement between calculation and our measurements.

In the present investigation, we used a standard model (Lam and Bremhorst, 1981), but we retained the acceleration terms appearing in the turbulence transport equations and we used $C_3 = 4.44$ as originally given by Hanjalic and Launder (1980). If the turbulence structure is assumed to be similar to the structure of a fully turbulent zero pressure gradient boundary layer, the wall heat flux is predicted very well.

Film Cooling. In the case of film cooling there is no influence of the throat on the cooling film stability. It should be pointed out that an injection mass flow ratio of only $\dot{m}_c/\dot{m} = 2.1$ percent (Table 3) yielded a significant decrease in heat transfer as well in the subsonic as in the supersonic region. An approximate comparison of mass flow ratios for axisymmetric nozzles may be obtained with simple geometry relations.

Table 1 Mainstream conditions

Symbol	O	Δ	□	◇	
$\dot{m}$	1.971	2.221	2.457	2.695	kg/s
p_o	190329	217227	242624	268616	Pa
T_o	447.4	458.6	467.8	476.3	K
u	55.34	56.02	59.02	59.60	m/s
T_w	309.5	309.5	318.0	323.0	K

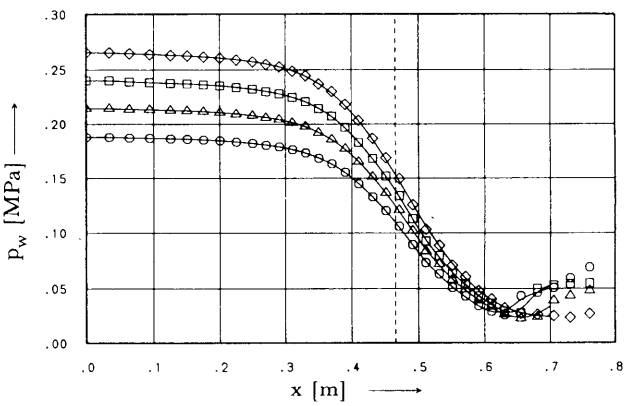

Fig. 4 Wall pressure $p_w(x)$ along plane nozzle wall

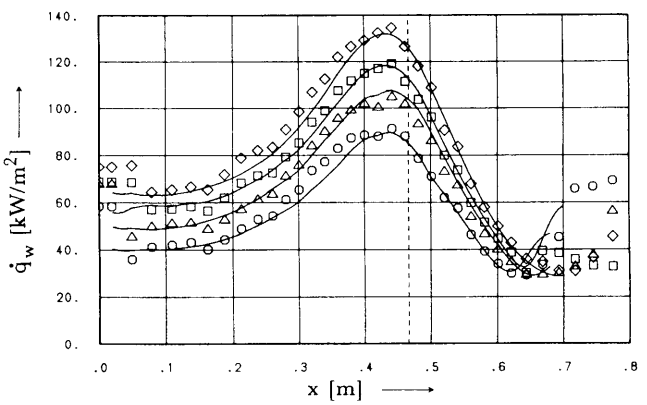

Fig. 5 Wall heat flux $\dot{q}_w(x)$; ◇, □, △, ○ measurements; ——— finite difference calculation

The calculated results are fairly good but not yet fully satisfactory for all injection rates. In contrast to the standard models predicting the wall heat flux again too small, the model with the additional acceleration terms overpredicts the heat transfer in the throat region for high injection rates.

Turbulence Model. The calculations are very sensitive to the choice of the additional constant and C_3 should be finally fixed from comparison of predictions with experiments for many different accelerated flow cases. Assumed the turbulence structure is described well with equations (33) and (34), the overprediction of heat transfer for high injection rates indicates that the constant $C_3 = 4.44$ as originally given by Hanjalic and Launder (1980) might be too big.

Since acceleration acts in a different way on $\widetilde{u''u''}$ and $\widetilde{v''v''}$ it might also be necessary to examine the structure of accelerated boundary layers and mixing layers experimentally and to use a complete Reynolds stress model. Additionally it will be necessary to develop a $\widetilde{v''T''}$ equation for accelerated flows and to prove the concept of a turbulent Prandtl number. Finally it is important to improve the standard models in comparison with experiments in zero pressure gradient, large density ratio boundary layers.

Table 2 Injection conditions for mainstream mass flow; $O\dot{m} = 1.971$ kg/s, slot height $s = 5 \times 10^{-3}$ m

Symbol (figs.6,7)	X	Y	Z	
$\dot{m}_c$	0.084	0.059	0.045	kg/s
$\dot{m}_c/\dot{m}$	4.3	3.0	2.3	%
$\frac{(\varrho u)_c}{\varrho u}$	2.12	1.49	1.13	
$\frac{(\varrho uu)_c}{\varrho uu}$	2.88	1.45	0.84	
u_c/u	1.36	0.97	0.75	
u_c	75.3	53.8	41.3	m/s
T_c	293.3	296.6	298.1	kg/s
T_c/T	0.66	0.67	0.67	

Table 3 Injection conditions for mainstream mass flow; $\Delta\dot{m} = 2.221$ kg/s, slot height $s = 5 \times 10^{-3}$ m

Symbol (figs.8,9)	X	Y	Z	
$\dot{m}_c$	0.081	0.055	0.046	kg/s
$\dot{m}_c/\dot{m}$	3.7	2.5	2.1	%
$\frac{(\varrho u)_c}{\varrho u}$	1.79	1.22	1.01	
$\frac{(\varrho uu)_c}{\varrho uu}$	2.04	0.97	0.67	
u_c/u	1.14	0.79	0.66	
u_c	64.4	44.4	37.2	m/s
T_c	300.4	302.6	303.8	K
T_c/T	0.66	0.66	0.66	

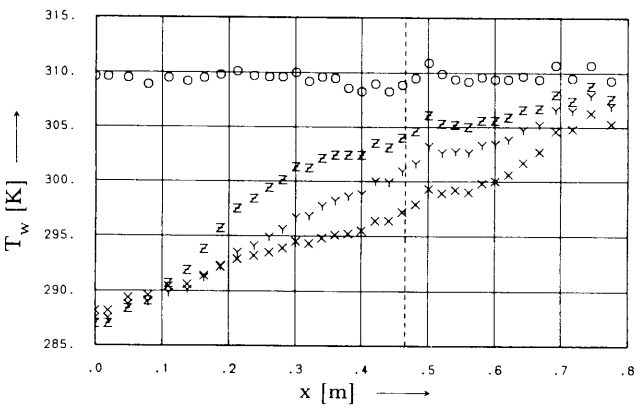

Fig. 6 Wall temperature $T_w(x)$ along plane nozzle wall

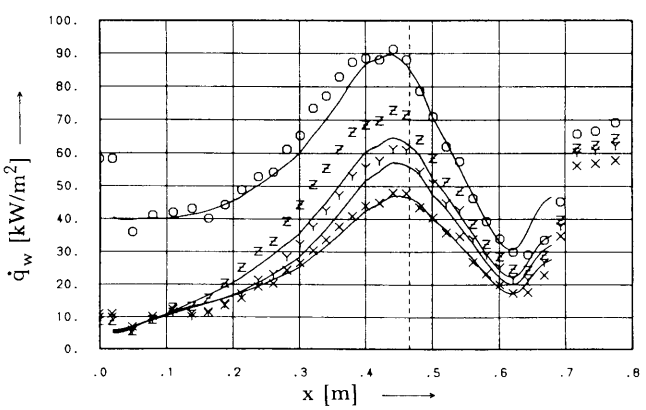

Fig. 7 Wall heat flux $\dot{q}_w(x)$; O,X,Y,Z measurements; _____ finite difference calculation

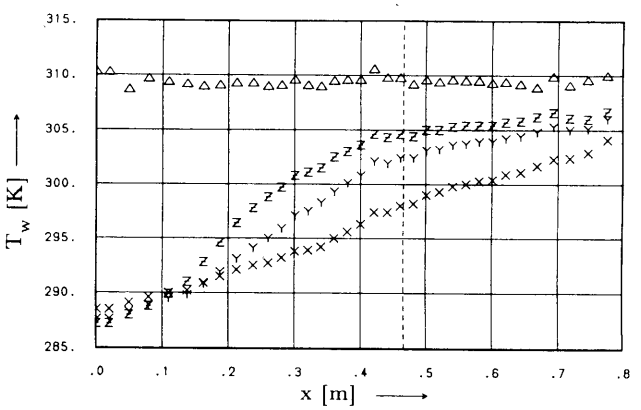

Fig. 8 Wall temperature $T_w(x)$ along plane nozzle wall

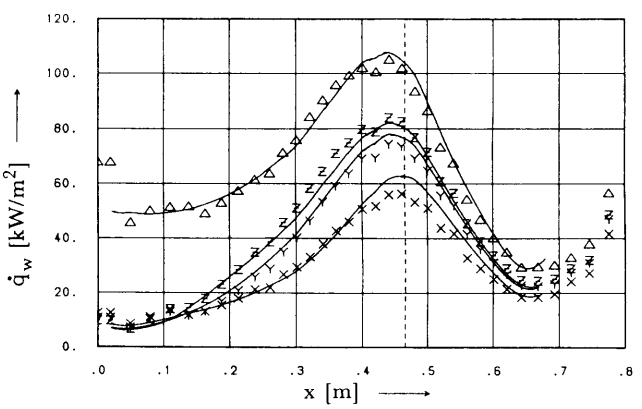

Fig. 9 Wall heat flux $\dot{q}_w(x)$; Δ,X,Y,Z measurements; _____ finite difference calculation

References

Abramovich, G. N., 1963, *The Theory of Turbulent Jets*, The M.I.T. Press, Massachusetts Institute of Technology, Cambridge, MA.

Back, L. H., Massier, P. F., and Gier, H. L., 1964, "Convective Heat Transfer in a Convergent-Divergent Nozzle," *Int. Journal Heat Mass Transfer*, Vol. 7, pp. 549-568.

Back, L. H., Cuffel, R. F., and Massier, P. F., 1970, "Laminarization of a Turbulent Boundary Layer in Nozzle Flow—Boundary Layer and Heat Transfer Measurements With Wall Cooling," ASME *Journal of Heat Transfer*, Vol. 92, pp. 333-344.

Back, L. H., and Cuffel, R. F., 1972, "Turbulent-Boundary-Layer Measurements Along a Supersonic Nozzle With and Without Wall Cooling," ASME *Journal of Heat Transfer*, Vol. 94, pp. 242-243.

Bauer, K., Winkler, W., and Grigull, U., 1978, "Heat Transfer in Compressible Turbulent Boundary Layer," *Proceedings International Heat Transfer Conference*, Toronto, Vol. 5, pp. 191-196.

Bauer, K., Straub, J., and Grigull, U., 1980, "Influence of Free-Stream Turbulence Intensity on Heat Transfer in the Two-Dimensional Turbulent Boundary Layer of an Accelerated Compressible Flow," *Int. Journal Heat Mass Transfer*, Vol. 23, pp. 1635-1642.

Boldman, D. R., Neumann, H. E., and Schmidt, J. F., 1967, "Heat Transfer in 30° and 60° Half-Angle Convergence Nozzles With Various Diameter Uncooled Pipe Inlets," NASA TN D-4177.

Boldman, D. R., and Graham, R. W., 1972, "Heat Transfer and Boundary Layers in Conical Nozzles," NASA TN D-6594.

Chambers, A. J., Antonia, R. A., and Fulachier, L., 1985, "Turbulent Prandtl Number and Spectral Characteristics of a Turbulent Mixing Layer," *Int. Journal Heat Mass Transfer*, Vol. 28, No. 8, pp. 1461-1468.

Chien, K.-Y., 1982, "Predictions of Channel and Boundary-Layer Flows With a Low-Reynolds-Number Turbulence Model," *AIAA Journal*, Vol. 20, p. 33.

Crawford, M. E., and Kays, W. M., 1976, "STAN5—a Program for Numerical Computation of Two-Dimensional Internal and External Boundary Layer Flows," NASA Contractor Report CR-2742.

Table 4 Injection conditions for mainstream mass flow; □ $\dot{m} = 2.457$ kg/s, slot height $s = 12 \times 10^{-3}$ m

Symbol (figs.10,11)	X	Y	Z	
$\dot{m}_c$	0.157	0.113	0.090	kg/s
$\dot{m}_c/\dot{m}$	6.4	4.6	3.6	%
$\frac{(\varrho u)_c}{\varrho u}$	1.25	0.90	0.71	
$\frac{(\varrho uu)_c}{\varrho uu}$	1.00	0.51	0.33	
u_c/u	0.79	0.57	0.46	
u_c	46.8	33.9	27.2	m/s
T_c	299.2	301.2	302.6	kg/s
T_c/T	0.64	0.65	0.65	

Table 5 Injection conditions for mainstream mass flow; ◇ $\dot{m} = 2.695$ kg/s, slot height $s = 12 \times 10^{-3}$ m

Symbol (figs.12,13)	X	Y	Z	
$\dot{m}_c$	0.149	0.115	0.087	kg/s
$\dot{m}_c/\dot{m}$	5.5	4.3	3.2	%
$\frac{(\varrho u)_c}{\varrho u}$	1.08	0.84	0.63	
$\frac{(\varrho uu)_c}{\varrho uu}$	0.73	0.44	0.25	
u_c/u	0.67	0.53	0.40	
u_c	40.2	31.3	23.7	m/s
T_c	299.5	300.9	302.4	kg/s
T_c/T	0.63	0.63	0.64	

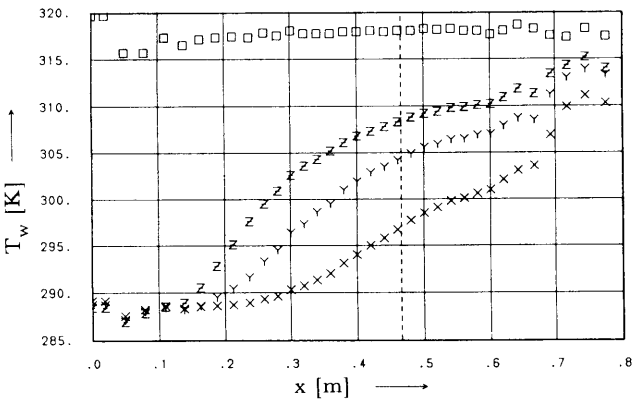

Fig. 10 Wall temperature $T_w(x)$ along plane nozzle wall

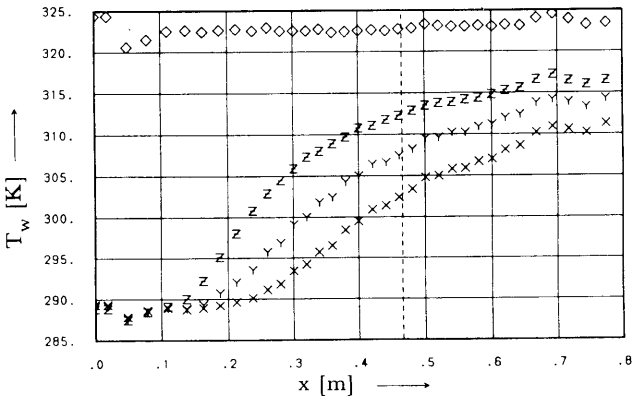

Fig. 12 Wall temperature $T_w(x)$ along plane nozzle wall

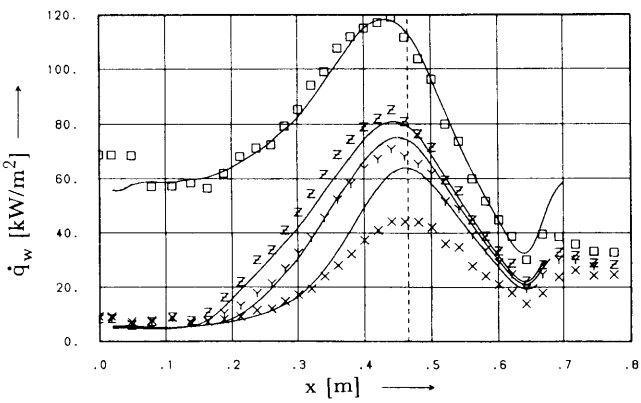

Fig. 11 Wall heat flux $\dot{q}_w(x)$; □,X,Y,Z measurements; _____ finite difference calculation

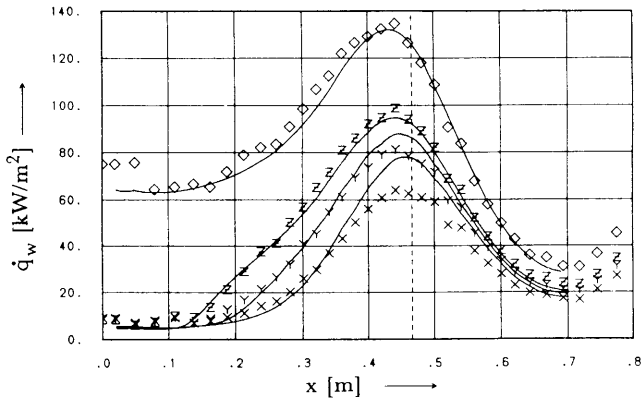

Fig. 13 Wall heat flux $\dot{q}_w(x)$; ◇,X,Y,Z measurements; _____ finite difference calculation

Crawford, M. E., 1986, "Lecture Series 1986-06: Convective Heat Transfer and Film Cooling in Turbomachinery," von Karman Institute for Fluid Dynamics, Brussels, Belgium.

Favre, A., 1965, "Equations des gaz Turbulent Compressible," Part I: *Journal de Mecanique*, Vol. 4, No. 3, pp. 361-390; Part II: *Journal de Mecanique*, Vol. 4, No. 4, pp. 391-421.

Favre, A., 1975, "Equations statistiques des fluides turbulents compressibles," *Proceedings Veme Congres canadien de Mecanique Appliquee*, New Brunswick, pp. G3-G34.

Fiedler, H. E., 1974, "Transport of Heat Across a Plane Turbulent Mixing Layer," *Adv. Geophys.*, Vol. 18, pp. 93-109.

Gibson, M. M., 1978, "An Algebraic Stress and Heat Flux Model for Turbulent Shear Flow With Streamline Curvature," *Int. Journal Heat Mass Transfer*, Vol. 21, pp. 1609-1617.

Hanjalic, K., and Launder, B. E., 1980, "Sensitizing the Dissipation Equation to Irrotational Strains," ASME *Journal of Fluids Engineering*, Vol. 102, pp. 34-40.

Hay, N., Lampard, D., and Saluja, C. L., 1985, "Effects of the Condition of the Approach Boundary Layer and of Mainstream Pressure Gradients on the Heat Transfer Coefficient on Film-Cooled Surfaces," ASME *Journal of Engineering for Gas Turbines and Power*, Vol. 107, pp. 99-110.

Hien, H. M., Vandromme, D. D., and MacCormack, R. W., 1980, "Comparison of Computation With Experiment," *ASFOSR-IFP Conference Proceedings*, Stanford.

Jones, T. V., and Forth, C. J. P., 1986, "The Scaling of Film Cooling—Theoretical and Experimental Results," Lecture Series 1986-06: *Convective Heat Transfer and Film Cooling in Turbomachinery*, von Karman Institute for Fluid Dynamics, Brussels, Belgium.

Jones, W. P., and Launder, B. E., 1972, "The Prediction of Laminarization With a Two Equation Model of Turbulence," *Int. Journal Heat Mass Transfer*, Vol. 15, pp. 301-314.

Julien, H. L., Kays, W. M., and Moffat, R. J., 1969, "The Turbulent Boundary Layer on a Porous Plate: Experimental Study of the Effects of a Favorable Pressure Gradient," Thermosciences Division Department of Mechanical Engineering, Stanford University, Report No. HMT-4.

Kays, W. M., Moffat, R. J., and Thielbar, W. H., 1970, "Heat Transfer to the Highly Accelerated Turbulent Boundary Layer With and Without Mass Addition," ASME *Journal of Heat Transfer*, Vol. 92, pp. 499-505.

Kebede, W., Launder, B. E., and Younis, B. A., 1985, "Large-Amplitude

Periodic Pipe Flow: A Second-Moment Closure Study," *Proc. 5th Turbulent Shear Flow Symposium*, Cornell University, pp. 16.23–16.29.

Klingbeil, E., 1966, *Tensorrechnung für Ingenieure*, Bibliographisches Institut AG, Mannheim.

Lam, C. K. G., and Bremhorst, K., 1981, "A Modified Form of the k–ϵ Model for Predicting Wall Turbulence," ASME *Journal of Fluids Engineering*, Vol. 103, pp. 456–460.

Ligrani, P. M., and Camci, C., 1985, "Adiabatic Film Cooling Effectiveness From Heat Transfer, Measurements in Compressible Variable-Property Flow," ASME *Journal of Heat Transfer*, Vol. 107, pp. 313–320.

Ljuboja, M., and Rodi, W., 1980, "Calculation of Turbulent Wall Jets With an Algebraic Reynolds Stress Model," ASME *Journal of Fluids Engineering*, Vol. 102, pp. 351–356.

Ljuboja, M., and Rodi, W., 1981, "Prediction of Horizontal and Vertical Turbulent Buoyant Wall Jets," ASME *Journal of Heat Transfer*, Vol. 103, pp. 343–349.

Norris, L., 1975, "Turbulent Channel Flow With a Moving Wary Boundary," Dissertation, Department of Mechanical Engineering, Stanford University, Stanford, CA.

Norris, L. H., and Reynolds, W. C., 1975, "Turbulent Channel Flow With a Moving Wary Boundary," Rept. No. FM-10, Department Mechanical Engineering, Stanford University, Stanford, CA.

Patankar, S. V., and Spalding, D. B., 1970, *Heat and Mass Transfer in Boundary Layers—A General Calculation Procedure*, Intertext Books, London.

Patel, V. C., Rodi, W., and Scheurer, G., 1985, "Turbulence Models for Near-Wall and Low Reynolds Number Flows: a Review," *AIAA Journal*, Vol. 23, No. 9, pp. 1308–1319.

Rodi, W., and Scheurer, G., 1983, "Scrutinizing the k–ϵ-Model Under Adverse Pressure Gradient Conditions," *Proc. 4th Turbulent Shear Flow Symposium*, Karlsruhe, Federal Republic of Germany.

Rodi, W., and Scheurer, G., 1985, "Calculation of Heat Transfer to Convection-Cooled Gas Turbine Blades," ASME *Journal of Engineering for Gas Turbines and Power*, Vol. 107, pp. 620–627.

Rotta, J. C., 1972, *Turbulente Strömungen—Eine Einführung in die Theorie und ihre Anwendungen*, B. G. Teubner, Stuttgart, Federal Republic of Germany.

Rued, K., and Wittig, G., 1985, "Free-Stream Turbulence and Pressure Gradient Effects on Heat Transfer and Boundary Layer Development on Highly Cooled Surfaces," ASME *Journal of Engineering for Gas Turbines and Power*, Vol. 107, pp. 54–59.

Thielbar, W. H., Kays, W. M., and Moffat, R. J., 1969, "The Turbulent Boundary Layer: Experimental Heat Transfer With Boiling, Suction, and Favourable Pressure Gradient," Thermosciences Division, Department of Mechanical Engineering, Stanford University, Report No. HMT-5.

Townsend, A. A., 1976, *The Structure of Turbulent Shear Flow*, Cambridge University Press, Great Britain.

Vandromme, D. D., and Minh, H. H., 1984, "Solution of the Compressible Navier-Stokes Equations: Applications to Complex Turbulent Flows," Lecture Series 1984-04: *Computational Fluid Dynamics*, von Karman Institute for Fluid Dynamics, Brussels, Belgium.

Wang, T., Simon, T. W., and Buddhavarapu, J., 1985, "Heat Transfer and Fluid Mechanics Measurements in Transitional Boundary Layer Flows," ASME *Journal of Engineering for Gas Turbines and Power*, Vol. 107, pp. 1007–1015.

Wilcox, D. C., and Rubesin, M. W., 1980, "Progress in Turbulence Modeling for Complex Flow Fields Including Effects of Compressibility," NASA TP 1517.

Winkler, W., and Grigull, U., 1977, "Wärmeübergang turbulenter kompressibler Grenzschichtströmungen mit starken negativen Druckgradienten (Wärmeübergang in einer Lavaldüse)," *Wärme- und Stoffübertragung*, Vol. 10, pp. 281–291.